Biodesign

pISSN 2288-6982 | eISSN 2288-7105

MINI REVIEW P 15-22

Time-resolved serial femtosecond X-ray crystallography

Ji-Hye Lee[1], Nadia A. Zatsepin[2,3] and Kyung Hyun Kim[1]*

[1]Department of Biotechnology & Bioinformatics, Korea University, Sejong 30019, Korea, [2]Department of Physics, Arizona State University, Tempe, AZ, U.S.A, [3]Biodesign Center for Applied Structural Discovery, Arizona State University, Tempe, AZ, U.S.A

*Correspondence: nadia.zatsepin@asu.edu; khkim@korea.ac.kr

Time-resolved serial femtosecond crystallography (TR-SFX) with X-ray free electron lasers (XFELs) is a powerful new technique for the study of protein dynamics on unprecedented time scales, at room temperature, without structure-affecting radiation damage. The construction of Pohang Accelerator Laboratory XFEL, a 0.1-nm hard X-ray free-electron laser facility based on a 10-GeV S-band linear accelerator in Pohang, Korea, provides a great opportunity to exploit and develop this novel methodology for structural biological studies. This review summarizes the state of the art in TR-SFX including key contributions of pump-probe and mix-and-inject TR-SFX to the field of protein dynamics.

INTRODUCTION

The invention of self-amplified spontaneous emission (SASE) mode hard X-ray free electron lasers (XFELs) has produced unprecedented opportunities for physics, chemistry, materials science, and biology (Spence, 2017). Current XFELs generate extremely intense, highly coherent, collimated X-ray pulses with femtosecond (fs) duration, with a beam diameter focused to 0.1 – 2 microns (Patterson et al., 2010; Yabashi et al., 2015; Bostedt et al., 2016; Park et al., 2016; Ko et al., 2017; Tschentscher et al., 2017). The ultrabrief X-ray pulses contain approximately 10^{12} photons, offering extremely high peak brilliance, roughly 10 orders of magnitude greater than that of a synchrotron X-ray pulse (Ansari et al., 2005). The commissioning of the first hard XFEL, the Linac Coherent Light Source (LCLS) at SLAC National Accelerator Laboratory (Menlo Park, CA, USA) in 2009, was followed by the publication of an exponentially increasing number of high-impact papers exploiting the novel modalities and strong diffraction signals offered by the XFEL, to learn more about molecular machines and mechanisms in life.

Synchrotron X-ray crystallography is a well-established approach to obtaining high-resolution protein structures based on large, good quality protein crystals. However, a bottleneck of synchrotron-based experiments lies in radiation damage accumulated from the long exposures necessary to collect sufficient scattering intensity, photoreduction of metalloproteins (Berglund et al., 2002; Schlichting et al., 2000), and the long pulse durations limiting the temporal resolution of time-resolved studies. An additional drawback is the frequent requirement to work on cryo-frozen samples (to significantly slow down radiation damage), which necessitates finding a suitable cryo-protectant and can bias structural ensembles in protein crystals (Spence et al., 2012). Cryo-crystallography therefore precludes the ability to study protein motions such as catalysis mediated by enzyme–substrate complexes, ligand binding and allosteric regulation (Fraser et al., 2009, 2011; Spence et al., 2012; Keedy et al. 2014; Fukuda and Inoue, 2015) at near-physiological temperature.

Femtosecond X-ray pulses enable the diffraction-before-destruction mode of data collection where the diffraction data are read out before the onset of structure-altering radiation damage, which is traditionally the major limitation on data quality in synchrotron-based protein crystallography and high-resolution biological imaging, particularly at room temperature (Neutze et al., 2000; Barty et al., 2011; Chapman et al., 2011; Nogly et al., 2014). In addition, the extreme brilliance of XFELs allows high resolution diffraction data to be collected even from very small volumes of micro- or nanocrystals, which more readily form monocrystals (Mizohata et al., 2017), and thus alleviates the requirement for large, high-quality biological crystals (Gati et al., 2017). The sample is destroyed after a single XFEL pulse, so various methods have been developed to rapidly replenish the sample including spraying/injecting a continuous stream of microcrystals in a liquid or lipidic jet (DePonte et al., 2008; Weierstall et al., 2014), or raster-scanning a fixed target across the pulsed XFEL beam (Roedig et al., 2017). This novel crystallographic technique, serial femtosecond crystallography (SFX), opened a new era in structural biology (Spence, 2017) by enabling protein dynamic studies. Dynamics is an essential aspect of protein structure and function. The ultimate goals in biophysics and structural biology are to elucidate molecular dynamics at atomic resolution at room temperature, in the native physiological environment of the target (e.g. proteins).

SFX IN STRUCTURAL BIOLOGY

SFX involves the collection of snapshot diffraction patterns

from randomly oriented microcrystals streamed across the XFEL beam with exposure time typically on the order of 20-50 fs (Chapman et al., 2011). However, SASE XFEL pulses fluctuate in intensity and spectrum, and microcrystals naturally exhibit variations in crystal size and morphology, all of which contribute to error in the merged diffracted intensities. Without accurate modelling of the scattering (scaling and post-refinement of the partial reflections measured from randomly oriented microcrystals), simply averaging the equivalent reflections in the snapshot diffraction patterns effectively performs a Monte Carlo integration over these randomly distributed variables (beam and crystal fluctuations), so the total error is inversely proportional to the square root of the number of diffraction patterns (Kirian et al., 2011; Li et al., 2015). As a result, thousands to tens of thousands of diffraction patterns are needed to obtain high-quality X-ray data in SFX (Tenboer et al., 2014, Barends et al., 2015).

Highlights from the first 8 years of SFX studies include the determination of high-resolution structures of protein nanocrystals grown in vivo within cells (Arnlund et al., 2011; Redecke et al., 2013) and numerous G protein-coupled receptors (GPCRs), an important class of membrane proteins crucial for drug development and rational drug design (Johansson et al., 2017). Large membrane proteins and protein complexes are particularly difficult to crystallize with sufficient crystal size and quality for synchrotron structure determination. In fact, the structures of a number of GPCRs with their bound ligand drug molecules could only be determined using an XFEL (Liu et al., 2013; Fenalti et al., 2014; Kang et al., 2015). While the development of SFX technology and software has been rapid, the reach of the technique has been limited by highly competitive, scarce XFEL beamtime due to a very small number of operational XFELs worldwide. The addition of recently built and upcoming XFEL facilities, including PAL-XFEL, has the potential for great impact in science and beyond.

XFEL sources

Currently, there are only five hard X-ray laser facilities operating in the world, the LCLS at SLAC in USA (Bostedt et al., 2016), SPring-8 Angstrom Compact free electron Laser (SACLA) in Japan (Yabashi et al., 2017), the Pohang Accelerator Laboratory X-ray Free-Electron Laser (PAL-XFEL) in Korea (Park et al., 2016; Ko et al., 2017), the European XFEL (EuXFEL) in Germany (Tschentscher et al., 2017) and SwissFEL in Switzerland (Patterson et al., 2010), with more under construction. The basic operating principle of a SASE FEL is the emission of radiation from relativistic electron beams travelling through an alternating periodic magnetic field (Margaritondo & Rebernik Ribic, 2011). The characteristic of a SASE FEL is the transition from noise (in the electron bunch) to an ordered state (electron bunches organized into microbunches separated by one radiation wavelength), which leads to the emitted radiation intensity scaling with the square of the number of electrons. This intensity amplification provides the massive increase in flux at the 4th generation X-ray sources. The current and upcoming hard X-ray FEL characteristics from various facilities are summarized in Table 1. For example, the LCLS provides about 1x10^{12} photons at 120 Hz repetition rate into a focused spot as small as 0.1 μm diameter, based on the maximum electron energy of 15 GeV.

In PAL-XFEL, the installation of the 10-GeV Linac, with undulators and beamlines, was completed by 2015. The commissioning and the first lasing of the hard X-ray FEL line were achieved in 2016 (Ko et al., 2017). The PAL-XFEL started user service in 2017, followed by user-assisted commissioning beamtimes at EuXFEL and the first pilot experiments at SwissFEL in late 2017. The EuXFEL generates high-luminosity X-rays at a repetition rate of 27,000 pulses per second. To exploit this, the Adaptive Gain Integrating Pixel Detector was designed to read out ~3,500 pulses per second (in 10 Hz pulse trains with pulses separated by 220 ns), potentially enabling the collection of a complete SFX dataset in less than 10 seconds (Marx, 2017). Due to the small number of XFEL experiments that can be performed concurrently at any XFEL, however, the slowly increasing number of XFEL facilities still does not meet the needs of the global user community and XFEL beamtime will continue to be highly

TABLE 1 | Hard X-ray free electron laser facilities

	SLAC		SACLA (Spring-8)	PAL-XFEL	European XFEL	SwissFEL
	LCLS-I	LCLS-II				
Construction period	2005-2008	2010-2018	2007-2011	2011-2016	2011-2016	2013-2016
Maximum electron energy (GeV)	15	2-15	8.5	10	17.5	6
Wavelength (nm)	4.6-0.11	7.7-0.05	6-0.08	6-0.1	6-0.08	10-0.1
Repetition rate (per second)	120 Hz	1 MHz	60 Hz	60 Hz	10 Hz pulse trains (4.5 MHz pulses)	100 Hz
Year completion	2009	2018	2011	2016	2017	2017

competitive and oversubscribed. With the advent of PAL-XFEL, EuXFEL and SwissFEL, we have an important opportunity to form productive new international collaborations and broaden the impact of XFEL technology on structural biology research worldwide.

Sample injectors and carrier matrices

The Gas Dynamic Virtual Nozzle (GDVN) injector was one of the first sample injectors for SFX experiments (DePonte et al., 2008). The liquid stream of microcrystals, focused by a concentric sheath of gas, had typical flow rates of 10–40 μL/min, resulting in a high rate of sample consumption with most of the sample wasted between XFEL shots. An injector for high-viscosity media was later developed, originally for membrane proteins crystallized in lipidic cubic phase (LCP) (Weierstall et al., 2014). Due to a 100–1,000 fold slower flow rate, the LCP injector wastes orders of magnitude less protein, reducing sample consumption for structure determination to as little as 0.3 mg of protein per data set (Liu et al., 2013). The LCP injector and similar systems can also be used for soluble protein microcrystal delivery using a variety of viscous media (Conrad et al., 2015; Sugahara et al., 2015; 2017), including monoolein (Wallace et al., 2011; Liu et al., 2013), agarose (Conrad et al., 2015), grease (Sugahara et al., 2015), and hydrogels such as sodium carboxymethyl cellulose and Pluronic F-127 (Kovacsova et al., 2017). Additionally, nanoelectrospinning of the liquid in a vacuum with a flow rate of 0.2–3 μl/min (Sierra et al., 2012), raster scanning a fixed-target sample holder (Cohen et al., 2014; Hunter et al., 2014; Roedig et al., 2015), and on-demand acoustic droplet generation (Mafune et al., 2016; Roessler et al., 2016) were developed, similarly requiring much lower sample consumption than the original GDVN jets. GDVN designs have also improved significantly, with thinner, more stable liquid jets (< 1 μm diameter), likewise reducing sample consumption (Oberthuer et al., 2017). Importantly, a stable sample stream was critical to obtain accurate measurement during data collection for SFX (Nango et al., 2016).

TIME RESOLVED-SFX

Synchrotron time-resolved (TR) experiments revealed that large structural changes occur in times shorter than 100 ps (Schotte et al., 2003, 2012; Bourgeois et al., 2006; Schmidt, M. 2013), a timescale inaccessible to synchrotron-based experiments. Accessing femtosecond or few-picosecond timescales, made possible by XFELs, will elucidate the intermediates adopted by proteins and how the conformational changes correlate with the different stages of biological functions (Moffat, 2014). SFX using fs pulses from XFEL sources enables ultrafast TR structural studies, allowing the structure determination of reaction intermediates (Chapman et al., 2011; Aquila et al., 2012; Neutze et al., 2012; Spence et al., 2012; Tenboer et al., 2014, Barends et al., 2015; Pande et al., 2016; Coquelle et al., 2017).

TR-SFX at XFEL is able to monitor reversible or irreversible conformational changes because the microcrystals are discarded after only one X-ray shot (Schmidt et al., 2013). However, each time delay (each frame in a 'molecular movie') requires hundreds to thousands of crystals for reliable structure factors at high resolution. PAL XFEL can deliver hard XFEL pulses at up to 60 Hz, and with serial sample delivery, each XFEL pulse can, in principle, be used to obtain a diffraction pattern from nanocrystals or potentially individual biomolecules.

Pump-probe approach

TR-SFX is an innovative method that enables us to observe how protein structures change while functioning. TR-SFX techniques have opened a new era of study of protein structural dynamics and provide unprecedented data for understanding protein functions. As opposed to the trapping experiments, in which structures in thermal equilibrium are trapped, pump-probe experiments involve proteins photo-activated by pump lasers and their diffraction patterns then probed by ultrafast X-ray pulses (Spence, 2017). The time delay between photoactivation and X-ray interaction is mainly determined by the pump laser duration and the flow rate in the stream (Figure 1). Steady improvements in data collection and analysis in TR-SFX experiments on nano- to micron-sized crystals have ensured that small structural

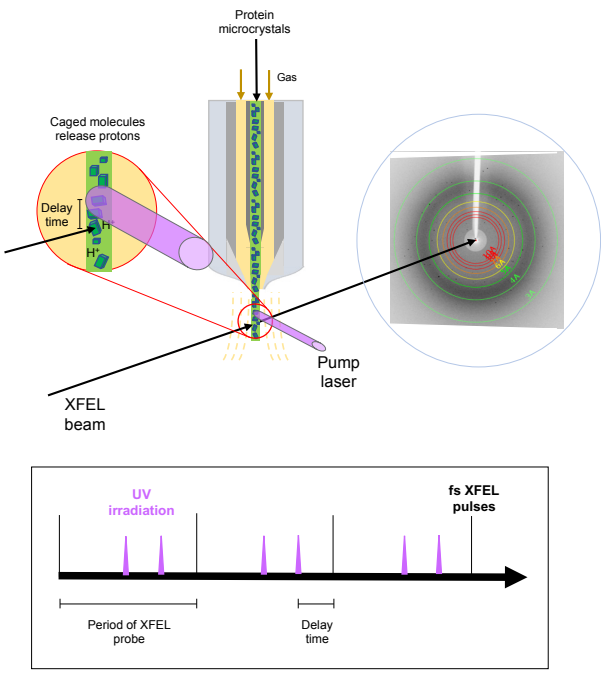

FIGURE 1 | Schematic of a pump-probe time-resolved serial femtosecond crystallography experiment using light-activated caged molecules for rapid pH change. Femtosecond X-ray pulses are focused on a stream of protein microcrystals. The insert shows the pump laser intersects the stream of microcrystals upstream of the X-ray pulse. The delay time is set by the distance between pump and probe along the crystal-laden liquid jet divided by flow rate. The box below shows a timeline of pump laser-induced photoactivation. The microcrystals are activated by pump laser prior to the interaction with the X-ray pulse and diffraction data are collected after the delay time.

changes can be resolved, despite the variations in XFEL pulses, crystal size and orientation.

Typically, laser pulses used in pump-probe experiments at synchrotrons photoactivate ~ 10-40% of the molecules in a fixed sample (Tenboer et al., 2014). In SFX, however, the microcrystals (smaller than the extinction length of the pump laser) allow uniform laser initiation of the reaction in the whole crystal (Table 2). TR-SFX of cis/trans isomerization in photoactive yellow protein (PYP) at delay times of 10 ns and 1 μs resulted in difference electron density maps in the chromophore pocket that were more easily interpretable than the corresponding Laue time-resolved crystallography data, allowing clear visualization of structural intermediates, thus greatly improving protein dynamics studies (Tenboer et al., 2014). Subsequent pump-probe TR-SFX at shorter time delays showed structural changes associated with the earliest steps in the PYP chromophore isomerization, revealing a snapshot series of intermediates over a time range from 100 fs to 3 ps (Pande et al., 2016).

High-resolution structures of photosystem II, a large membrane protein complex involved in photosynthesis in plants and algae, provided new insights into water oxidation. A detailed mechanism for the O=O bond formation was suggested based on damage-free intermediate structures from pump-probe TR-SFX at both cryogenic and room temperatures (Young et al., 2016; Suga et al., 2017).

In the carbonmonoxy myoglobin complex, photolysis-driven structural changes were resolved in over pump-probe delays range of 100 fs–500 ps (Barends et al., 2015). The photodissociation of the Fe-CO bond was found to induce ultrafast modes of local conformational changes at the heme binding site, observed at sub-ps time delays, and large-scale motions were essentially complete after 150 ps. At ultrafast time scales, protein motions are local and often involve only chromophore or amino acid side chains. In contrast, motions on slower time scales (ns to ms) might involve larger conformational changes.

Light-induced structural changes have also been imaged in a number of other protein model systems (Table 2), including P450 nitric oxide reductase, reaction center, bacteriorhodopsin, a light-driven proton pump derived from *Halobacterium salinarum*, and green fluorescent protein (Arnlund et al., 2014; Nango et al., 2016; Coquella et al., 2017; Suga et al., 2017; Tosha et al., 2017).

Mix-and-inject approach

The fast timescales of biochemically relevant processes range from fs to ms, which TR-SFX experiments are designed to match. While photoactivated reactions are focused on ultrasfast steps occurring on fs–ns timescales, large-scale conformational changes associated with ligand binding or by pH or temperature jump occur in μs–ms. In this context, ultrafast TR experiments have been mostly carried out in solution using spectroscopic probes rather than in crystals, and Laue diffraction in crystals

TABLE 2 | Pump-probe conditions in recent TR-SFX experiments

Target proteins*	PSII	PSII	PYP	PYP	$P450_{nor}$	RC_{vir}	MbCO	bR	rsEGFP
Pulse energy	2.3 mJ/cm^2	21-52 mJ/cm^2	~800 μJ/mm^2	0.75 mJ./cm^2	0.31–0.51 nJ/μm^2	5.3 mJ/mm^2	900 μJ/mm^2	>800 μJ/mm^2	940 μJ/mm^2
Pulse width (duration)	90 ns, 150 ns	7 ns	>100 μs	100 fs- 3 ps	6 ns	0.5 ps	0.5 ps	4 ns	230 fs
Delay time	210 μs	10 ms, 20 ms	10 μs – 1 μs	100 fs – 3 ps (300 fs, 600 fs)	>16.7 ms	0-280 ps	0.5 – 150 ps (0.5 ps interval)	16 ns–1.7 ms	1ps, 3ps
Repetition**	60 Hz	10 Hz	40 Hz	120 Hz	10 Hz	60 Hz	1 kHz	15 Hz (10 Hz)	10 Hz
Wavelength	527 nm	532 nm	450 nm	450 nm	308 nm	800 nm	538 nm	532 nm	532 nm
Focal size	400 μm	240 μm	150 μm	140±10 μm	250 μm	250 μm	150 μm	40 μm	40 μm
Microcrystal size	1-2 μm	100 μm	~ 5 μm	~ 5 μm	20-50 μm	solution	15×5×3 μm^3		~ 3 μm
Flow rate	2.8-5.6 μl/min	2.8-5.6 μl/min	22-25 μl/min	22-25 μl/min	4.6 mm/s	10 μl/min	~30 μl/min	2.5 μl/min (1.0 μl/min)	2.8-5.6 μl/min
Frequency**	120 Hz	30 Hz	120 Hz	120 Hz	30 Hz	120 Hz	120 Hz	30 Hz	30 Hz
XFEL facility	LCLS	SACLA	LCLS	LCLS	SACLA	LCLS	LCLS	SACLA	LCLS
Reference	Kupitz et al., 2014	Suga et al., 2017	Tenboer et al., 2014	Pande et al., 2016	Tosha et al., 2017	Arnlund et al., 2014	Barends et al., 2015	Nango et al., 2016	Coquelle et al., 2017

*Abbreviations: PYP, photoactive yellow protein; $P450_{nor}$, nitric oxide reductase (nor) isolated from the fungus Fusarium oxysporum; RC_{vir}, Blastochloris viridis photosynthetic reaction center; MbCO, carbonmonoxy myoglobin; bR, Bacteriorhodopsin; PSII, Photosystem II, rsEGFP, reversibly photoswitchable fluorescent protein. **Repetition and frequency refer to collection of pumped data only and total, respectively.

has thus been used for probing structural changes of proteins in light-driven photochemical reactions (Moffat 2001, 2014). However, not many proteins show structural changes induced by light. A different type of reaction trigger was developed, mixing with a ligand or a substrate, for so-called mix-and-inject serial crystallography (MISC) in riboswitch RNA (Stagno et al., 2017) and in β-lactamase (Kupitz et al., 2017). MISC is a technique designed to capture images of enzyme-catalyzed reactions in which protein microcrystals are mixed with a substrate then probed by an X-ray pulse (Schmidt, 2013). Thus MISC, as a convenient reaction initiation, opens a new field of TR-SFX for substrate or ligand-triggered biological reactions. The time-resolution in MISC depends on the diffusion of the substrate into the microcrystals, limiting the time resolution that can be achieved with large crystals. The dynamics and activity of most enzymes and RNA occur in ms timescale (Wolf-Watz et al., 2004; Al-Hashimi et al., 2008), whereas diffusion into crystals smaller than about a 10 μm^3 volume is on the sub-ms timescale (Schmidt, 2013), which is also faster than characteristic lifetimes of the structural intermediates in conformational changes. Starting an enzymatic reaction by allowing a substrate to diffuse into the crystal thus benefits from the small size of microcrystals used in XFEL-based SFX due to their much larger surface-to-volume ratio (than in big crystals). In addition, compared to the single large crystals, microcrystals show less crystal disorder induced by osmotic shock during soaking (Mizohata et al., 2017).

To trigger an enzymatic reaction with MISC necessitated the invention of mixing jets that can provide rapid mixing times. Mixing jet devices were initially developed that were capable of mixing two liquids inside a nozzle and then injecting them as a free jet into vacuum to achieve fast mixing (Wang et al., 2014; Calvey et al., 2016). In the case of the riboswitch RNA, a T-junction based mixer capable of delay times of a few seconds was used to capture the structure of a ligand-bound intermediate after a 10 s delay (Stagno et al., 2017). A system combining a polyimide tape drive and microfluidic mixers was also developed for mix-and-diffuse serial crystallography at a synchrotron, demonstrated with ligand binding in lysozyme within 2 s (Beyerlein et al., 2017). After mixing with the protein microcrystals, nearly full occupancy of the ligand was observed, indicating that the mix-and-diffuse approach has the potential for high-throughput drug screening on short timescales (Beyerlein et al., 2017).

Importantly, many proteins require alternative physical triggers to initiate reactions such as a pH jump, temperature jump, or THz-radiation (Neutze & Moffat, 2012; Moffat, 2014), for which alternative approaches are being developed.

Caged molecule-mediated pH jump approach

It is difficult to initiate enzymatic reactions on μs or shorter timescales using current mixing jet technology. The reaction time points accessible to current mixer technology have a limit of 10 ms - 2 s. Although ultrafast reactions could be observed using a liquid jet injector, in which microcrystals travel very fast in the jet (typical flow speed ca. 10 m/s), the range of available delay times is currently limited. Alternatively, photo-activated caged molecules mixed with microcrystals can induce conformational changes of proteins or enzymatic reactions. Recent development of a nanosecond optical-pump probe device for TR-SFX at SACLA achieved high excitation efficiency of protein nanocrystals by pump illumination, in which delay times after photo-excitation are accessible from ns to ms, currently limited to approximately 20 ms to 7 ns (Suga et al., 2017).

The conformational changes of proteins initiated by acidic pH are difficult to monitor by TR-SFX, and a method of inducing a caged-molecule-driven pH jump is essential to the success of pH induced protein dynamics studies. The caged molecule-driven pH jump methodology will be particularly critical in obtaining systematic measurements of the conformational changes in the protein microcrystals, when the available mixing jet technology is unable to provide the necessary time frames for TR-SFX measurements. In order to identify the conditions under which a substantial fraction of protein molecules would have embarked on a series of conformational changes, reliable caged molecule-driven pH-controlled experiments are needed.

Ortho-nitrobenzaldehyde (*o*-NBA) has been used as one of the proton cage molecules to investigate pH-controlled dynamics of proteins (Causgrove et al., 2006). *o*-NBA is excited to a reactive state by UV irradiation (typically 266 nm or 355 nm), which results in the release of protons that is faster than rapid exchange of solution, to create a pH jump within the microcrystals (Donten et al., 2011). Previous microfluidic experiments showed that irradiation with a 4 mW UV laser dropped the pH of the solution of proteins immobilized in microchannels, resulting in successful pH decrease from 7.0 to 5.0 in the ms time range (Costello et al., 2012). To prove the pH jump, single-virion fusion events were monitored using fluorescence microscopy, which revealed that protons were diffused to the bound viruses for successful membrane fusion. The caged molecule-driven pH jump is adaptable to studies of many biological processes including viral membrane fusion and cell fusion. The impact of this physical triggering platform, when established reliably, will be enormous from a practical standpoint in TR-SFX.

FUTURE PROSPECT FOR TR-SFX

Pump-probe TR-SFX has enabled the determination of room-temperature, high-resolution structures of proteins at several orders of magnitude better time resolution than is possible at synchrotrons, without radiation damage, under native conditions. MISC has given rise to the field of enzyme-catalyzed protein dynamics and development of advanced mix-and-diffuse modes with caged molecules will also contribute to the determination of molecular movies of protein dynamics and to elucidation of protein functions in chronological order at a molecular level. This review highlighted achievements in studying protein dynamics using TR-SFX at XFEL facilities that have started to provide user

operations: LCLS, SACLA, PAL-XFEL and EuXFEL.

Looking ahead, the TR-SFX approach can also serve as a foundation for an efficient structure-based drug discovery, since the XFEL source enables access to room temperature protein structure, which represents more accurately the conformational ensemble of proteins in physiological conditions. Structure-based drug design has proven highly successful for target proteins: anti-HIV and anti-hepatitis C virus (HCV) drugs based on 3D structure of viral target enzymes. SFX will show the differences between such structures at room temperature and those with cryo-cooling and radiation damage. In addition, intermediate structures may expose ligand binding that has not yet been seen, so that different binding motifs can be screened. Importantly, micro- or nanocrystals allow for faster and more efficient ligand soaking and exchange. Since dynamics are an integral part of protein function, the use of SFX to determine structural details accurately at room temperature can make an important contribution to not only understanding the structure-function relationships, but also developing novel drug discovery.

CONFLICT OF INTEREST

The authors declare that they have no conflict of interest.

ACKNOWLEDGEMENTS

This work was supported by grants from the NRF funded by the Korean government (MSIP) (2016R1E1A1A01942558), BK21+ programs through NRF of the ME (K.H.K.), the Science and Technology Center Program of the National Science Foundation (NSF, USA) through BioXFEL under Agreement 1231306, and NSF ABI grant 1565180 (N.A.Z.).

REFERENCES

Ansari, A., Berendzen, J., Bowne, S.J., Frauenfelder, H., Iben, I.E.T., Sauke, T.B., Shyamsunder, E., and Young, RD. (2005). Protein states and proteinquakes. *Proc Natl Acad Sc USA* **82**, 5000-5004.

Al-Hashimi, H.M., and Walter, N.G. (2008). RNA dynamics: it is about time. *Curr Opin Struct Biol* **18**, 321-329.

Aquila, A., Hunter, M.S., Doak, R.B., Kirian, R.A., Fromme, P., White, T.A., Andreasson, J., Arnlund, D., Bajt, S., Barends, T.R., Barthelmess, M., Bogan, M.J., Bostedt, C., Bottin, H., Bozek, J.D., et al. (2012). Time-resolved protein nanocrystallography using an X-ray free-electron laser. *Opt Express* **20**, 2706-2716.

Arnlund, D., Johansson, L.C., Wickstrand, C., Barty, A., Williams, G.J., Malmerberg, E., Davidsson, J., Milathianaki, D., DePonte, D.P., Shoeman, R.L., Wang, D., James, D., Katona, G., Westenhoff, S., White, TA., et al. (2014). Visualizing a protein quake with time-resolved X-ray scattering at a free-electron laser. *Nat Methods* **11**, 923-926.

Barends, T.R., Foucar, L., Ardevol, A., Nass, K., Aquila, A., Botha, S., Doak, R.B., Falahati, K., Hartmann, E., Hilpert, M., Heinz, M., Hoffmann, M.C., Köfinger, J., Koglin, J.E., Kovacsova, G., et al. (2015). Direct observation of ultrafast collective motions in CO myoglobin upon ligand dissociation. *Science* **350**, 445-450.

Barty, A., Caleman, C., Aquila, A., Timneanu, N., Lomb, L., White, T.A., Andreasson, J., Arnlund, D., Bajt, S., Barends, T.R., Barthelmess, M., Bogan, M.J., Bostedt, C., Bozek, J.D., Coffee, R., et al. (2011). Self-terminating diffraction gates femtosecond X-ray nanocrystallography measurements. *Nat Photonics* **6**, 35-40.

Berglund, G.I., Carlsson, G.H., Smith, A.T., Szoeke, H., Henriksen, A., and Hajdu, J. (2002). The catalytic pathway of horseradish peroxidase at high resolution. *Nature* **417**, 463-468.

Beyerlein, K.R., Dierksmeyer, D., Mariani, V., Kuhn, M., Sarrou, I., Ottaviano, A., Awel, S., Knoska, J., Fuglerud, S., Jönsson, O., Stern, S., Wiedorn, M.O., Yefanov, O., Adriano, L., Bean, R., et al. (2017). Mix-and-diffuse serial synchrotron crystallography. *IUCr J* **4**, 769-777.

Bostedt, C., Boutet, S., Fritz, D.M., Huang, Z., Lee, H.J.,Lemke, H.T., Robert, A., Schlotter, W.F., Turner, J.J., Williams, G.J. (2016). Linac Coherent Light Source: The first five years. *Rev Mod Phy* **88**, 207. Bourgeois, D., Vallone, B., Arcovito, A., Sciara, G., Schotte, F., Anfinrud, P.A., and Brunori M. (2006). Extended subnanosecond structural dynamics of myoglobin revealed by Laue crystallography. *Proc Natl Acad Sci USA* **103**, 4924-4929.

Calvery, G., Katz, A.M., Schaffer, C.B., and Pollack, L. (2016). Mixing injector enables time-resolved crystallography with high hit rate at X-ray electron lasers. *Struct Dyn* **3**, 054301.

Causgrove, T., and Dyer, R. (2006). Nonequilibrium protein folding dynamics: laser-induced pH-jump studies of the helix–coil transition. *Chem Phys* **323**, 2-10.

Chapman, H.N., Fromme, P., Barty, A., White, T.A., Kirian, R.A., Aquila, A., Hunter, M.S., Schulz, J., DePonte, D.P., Weierstall, U., Doak, R.B., Maia, F.R., Martin, A.V., Schlichting, I., Lomb, L., et al. (2011). Femtosecond X-ray protein nanocrystallography. *Nature* **470**, 73-77.

Cohen, A.E., Soltis, S.M., González, A., Aguila, L., Alonso-Mori, R., Barnes, C.O., Baxter, E.L., Brehmer, W., Brewster, A.S., Brunger, A.T., Calero, G., Chang, J.F., Chollet, M., Ehrensberger, P., Eriksson, T.L., et al. (2014). Goniometer-based femtosecond crystallography with X-ray free electron lasers. *Proc Natl Acad Sci USA* **111**, 17122-17127.

Conrad, C.E., Basu, S., James, D., Wang, D., Schaffer, A., Roy-Chowdhury, S., Zatsepin, N.A., Aquila, A., Coe, J., Gati, C., Hunter, M.S., Koglin, J.E., Kupitz, C., Nelson, G., Subramanian, G., et al. (2015). A novel inert crystal delivery medium for serial femtosecond crystallography. *IUCrJ* **2**, 421-430.

Coquelle, N., Sliwa, M., Woodhouse, J., Schirò, G., Adam, V., Aquila, A., Barends, T.R.M., Boutet, S., Byrdin, M., Carbajo, S., De la Mora, E., Doak, R.B., Feliks, M., Fieschi, F., Foucar, L., et al. (2018). Chromophore twisting in the excited state of a photoswitchable fluorescent protein captured by time-resolved serial femtosecond crystallography. *Nat Chem* **10**, 31-7.

Costello, D.A., Lee, D.W., Drewes, J., Vasquez, K.A., Kisler, K., Wiesner, U., Pollack, L., Whittaker, G.R., and Daniel, S. (2012). Influenza virus-membrane fusion triggered by proton uncaging for single particle studies of fusion kinetics. *Anal Chem* **84**, 8480-8489.

DePonte, D.P., Weierstall, U., Schmidt, K., Warner, J., Starodub, D., Spence, J.C.H., and Doak, R.B. (2008). Gas dynamic virtual nozzle for generation of microscopic droplet streams. *J Phys D Appl Phys*, **41**, 195505.

Donten, M.L., Hamm, P., and VandeVondele, J. (2011). A consistent picture of the proton release mechanism of oNBA in water by ultrafast spectroscopy and ab initio molecular dynamics. *J Phys Chem B* **115**, 1075-1083.

Fenalti, G., Zatsepin, N.A., Betti, C., Giguere, P., Han, G.W., Ishchenko, A., Liu, W., Guillemyn, K., Zhang, H., James, D., Wang, D., Weierstall, U., Spence, J.C., Boutet, S., Messerschmidt, M., et al. (2014). Structural basis for the bi-functional peptide recognition at human δ-Opioid receptor. *Nat Struct Mol Biol* **22**:265-268.

Fraser, J.S., Clarkson, M.W., Degnan, S.C., Erion, R., Kern, D., and Alber, T. (2009). Hidden alternative structures of proline isomerase essential for catalysis. *Nature* **462**, 669-673.

Fraser, J.S., van den Bedem, H., Samelson, A.J., Lang, P.T., Holton, J.M., Echols, N., and Alber, T. (2011). Accessing protein conformational ensembles using room-temperature X-ray crystallography. *Proc Natl Acad Sci USA* **108**, 16247-16252.

Fukuda, Y., and Inoue, T. (2015). High-temperature and high-resolution crystallography of thermostable copper nitrite reductase. *Chem Commun (Camb)* **51**, 6532–6535.

Gati, C., Oberthuer, D., Yefanov, O., Bunker, R.D., Stellato, F., Chiu, E., Yeh, S.M., Aquila, A., Basu, S., Bean, R., Beyerlein, K.R., Botha, S., Boutet, S., DePonte, D.P., Doak, R.B., et al. (2017). Atomic structure of granulin determined from native nanocrystalline granulovirus using an X-ray free-electron laser. *Proc Natl Acad Sci USA* **114**, 2247-2252.

Hunter, M.S., Segelke, B., Messerschmidt, M., Williams, G.J., Zatsepin, N.A., Barty, A., Benner, W.H., Carlson, D.B., Coleman, M., Graf, A., Hau-Riege, S.P., Pardini, T., Seibert, M.M., Evans, J., Boutet, S., et al. (2014). Fixed-target protein serial microcrystallography with an x-ray free electron

laser. *Sci Rep* **4**, 6026.

Johansson, L.C., Stauch, B., Ishchenko, A., and Cherezov, V. (2017). A bright future for serial femtosecond crystallography with XFELs. *Trends Biochem Sci* **42(9)**, 749-762.

Kang, Y., Zhou, X.E., Gao, X., He, Y., Liu, W., Ishchenko, A., Barty, A., White, T.A., Yefanov, O., Han, G.W., Xu, Q., de Waal, P.W., Ke, J., Tan, M.H., Zhang, C., et al. (2015). Crystal structure of rhodopsin bound to arrestin by femtosecond X-ray laser. *Nature* **523**, 561-567.

Keedy, D.A., van den Bedem, H., Sivak, D.A., Petsko, G.A., Ringe, D., Wilson, M.A., and Fraser, J.S. (2014). Crystal cryocooling distorts conformational heterogeneity in a model Michaelis complex of DHFR. *Structure* **22**, 899-910.

Kirian, R.A., White, T.A., Holton, J.M., Chapman, H.N., Fromme, P., Barty, A., Lomb, L., Aquila, A., Maia, F.R., Martin, A.V., Fromme, R., Wang, X., Hunter, M.S., Schmidt, K.E., and Spence, J.C. (2011). Structure-factor analysis of femtosecond microdiffraction patterns from protein nanocrystals. *Acta Crystallogr A* **67**, 131-140.

Ko, I., Kang, H.-S., He,o H., Kim, C., Kim, G., Min, C.-K., Yang, H., Baek S., Choi, H., Mun, G., Park, B., Suh, Y., Shin, D., Hu, J., Hong, J. et al. (2017). Construction and Commissioning of PAL-XFEL Facility. *Appl Sci* **7**, 479-411.

Li, C., Schmidt, K., and Spence, J.C.H. (2015). Data collection strategies for time-resolved X-ray free-electron laser diffraction, and 2-color methods. *Structural Dynamics* **2**, 041714.

Liu, W., Wacker, D., Gati, C., Han, G.W., James, D., Wang, D., Nelson, G., Weierstall, U., Katritch, V., Barty, A., Zatsepin, N.A., Li, D., Messerschmidt, M., Boutet, S., Williams, G.J., et al. (2013). Serial Femtosecond Crystallography of G Protein-Coupled Receptors. *Science* **342**, 1521-1524.

Kovácsová, G., Grünbein, M.L., Kloos, M., Barends, T.R.M., Schlesinger, R., Heberle, J., Kabsch, W., Shoeman, R.L., Doak, R.B., and Schlichting I. (2017). *Viscous hydrophilic injection matrices for serial crystallography. IUCrJ* **4**, 400-410.

Kupitz, C., Basu, S., Grotjohann, I., Fromme, R., Zatsepin, N.A., Rendek, K.N., Hunter, M.S., Shoeman, R.L., White, T.A., Wang, D., James, D., Yang, J.H., Cobb, D.E., Reeder, B., Sierra, R.G., et al. (2014). Serial time-resolved crystallography of photosystem II using a femtosecond X-ray laser. *Nature* **513**, 261-265.

Kupitz, C., Olmos, J.L. Jr., Holl, M., Tremblay, L., Pande, K., Pandey, S., Oberthür, D., Hunter, M., Liang, M., Aquila, A., Tenboer, J., Calvey, G., Katz, A., Chen, Y., Wiedorn, M.O., et al. (2017). Structural enzymology using X-ray free electron lasers. *Struct Dyn* **4**, 044003.

Mafuné, F., Miyajima, K., Tono, K., Takeda, Y., Kohno, J.Y., Miyauchi, N., Kobayashi, J., Joti, Y., Nango, E., Iwata, S., and Yabashi, M. (2016). Microcrystal delivery by pulsed liquid droplet for serial femtosecond crystallography. *Acta Crystallogr D Struct Biol* **72**, 520-523.

Margaritondo, G., and Rebernik Ribic, P. (2011). A simplified description of X-ray free-electron lasers. *J Synchrotron Radiat* **18**, 101-108.

Mizohata, E., Nakane, T., Fukuda, Y,. Nango, E., and Iwata, S. (2017) Serial femtosecond crystallography at the SACLA: breakthrough to dynamic structural biology. *Biophys Rev doi:* **10**.1007/s12551-017-0344-9.

Moffat, K. (2001). Time-resolved biochemical crystallography: a mechanistic perspective. *Chem Rev* **101**, 1569-1581.

Moffat, K. (2014). Time resolved crystallography and protein design: signalling photoreceptors and optogenetics. *Phil Trans R Soc B* **369**, 20130568.

Nango, E., Royant, A., Kubo, M., Nakane, T., Wickstrand, C., Kimura, T., Tanaka, T., Tono, K., Song, C., Tanaka, R., Arima, T., Yamashita, A., Kobayashi, J., Hosaka, T., Mizohata, E., et al. (2016). A three-dimensional movie of structural changes in bacteriorhodopsin. *Science* **354**, 1552-1557.

Neutze, R., Wouts, R., van der Spoel, D., Weckert, E., and Hajdu, J. (2000). Potential for biomolecular imaging with femtosecond X-ray pulses. *Nature* **406**, 752-757.

Neutze, R., and Moffat, K. (2012). Time-resolved structural studies at synchrotrons and X-ray free electron lasers: opportunities and challenge. *Curr Opin Struct Biol* **22**, 651-659.

Nogly, P., James, D., Wang, D., White, T.A., Zatsepin, N., Shilova, A., Nelson, G., Liu, H., Johansson, L., Heymann, M., Jaeger, K., Metz, M., Wickstrand, C., Wu, W., Båth, P., et al. (2014). Lipidic cubic phase serial millisecond crystallography using synchrotron radiation. *IUCrJ* **2**,168-176.

Oberthuer, D., Knoška, J., Wiedorn, M.O., Beyerlein, K.R., Bushnell, D.A., Kovaleva, E.G., Heymann, M., Gumprecht, L., Kirian, R.A., Barty, A., Mariani, V., Tolstikova, A., Adriano, L., Awel, S., Barthelmess, M., et al. (2017). Double-flow focused liquid injector for efficient serial femtosecond crystallography. *Sci Rep* **7**, 44628.

Pande, K., Hutchison, C.D., Groenhof, G., Aquila, A., Robinson, J.S., Tenboer, J., Basu, S., Boutet, S., DePonte, D.P., Liang, M., White, T.A., Zatsepin, N.A., Yefanov, O., Morozov, D., Oberthuer D., et al. (2016). Femtosecond structural dynamics drives the trans/cis isomerization in photoactive yellow protein. *Science* **352**, 725-729.

Park, J., Kim, S., Nam, K.-H., Kim, B., and Ko, I. (2016). Current status of the CXI beamline at the PAL-XFEL. *J Korean Phys Soc* **69**, 1089-1094.

Patterson, B.D., Abela, R., Braun, H.-H., Flechsig, U., Ganter, R., Kim, Y., Kirk, E., Oppelt, A., Pedrozzi, M., Reiche, S., Rivkin, L., Schmidt, Th., Schmitt, B., Strocov V.N., Tsujino, S., Wrulich, A.F. (2010). Coherent science at the SwissFEL x-ray laser. *New J Phys **12(3)***, 035012-17.

Redecke, L., Nass, K., DePonte, D.P., White, T.A., Rehders, D., Barty, A., Stellato, F., Liang, M., Barends, T.R.M., Boutet, S., Williams, G.J., Messerschmidt, M., Seibert, M.M., Aquila, A., Arnlund, D., et al. (2013). Natively inhibited Trypanosoma brucei cathepsin B structure determined by using an X-ray laser. *Science* **339**, 227-230.

Roedig, P., Ginn, H.M., Pakendorf, T., Sutton, G., Harlos, K., Walter, T.S., Meyer, J., Fischer, P., Duman, R., Vartiainen, I., Reime, B., Warmer, M., Brewster, A.S., Young, I.D., Michels-Clark, T., et al. (2017). High-speed fixed-target serial virus crystallography. *Nat Methods* **14**, 805-810.

Roedig, P., Vartiainen, I., Duman, R., Panneerselvam, S., Stübe, N., Lorbeer, O., Warmer, M., Sutton, G., Stuart, D.I., Weckert, E., David, C., Wagner, A., and Meents, A. (2015). A micro-patterned silicon chip as sample holder for macromolecular crystallography experiments with minimal background scattering. *Sci Rep* **5**, 10451.

Roessler, C.G., Agarwal, R., Allaire, M., Alonso-Mori, R., Andi, B., Bachega, J.F.R., Bommer, M., Brewster, A.S., Browne, M.C., Chatterjee, R., Cho, E., Cohen, A.E., Cowan, M., Datwani, S., Davidson, V.L., et al. (2016). Acoustic injectors for drop-on-demand serial femtosecond crystallography. *Structure* **24**, 631-640.

Schlichting, I., Berendzen, J., Chu, K., Stock, A.M., Maves, S.A., Benson, D.E., Sweet, R.M., Ringe, D., Petsko, G.A., and Sligar, S.G. (2000). The catalytic pathway of cytochrome P450cam at atomic resolution. *Science* **287**, 1615-1622.

Schmidt, M. (2013). Mix and inject: reaction initiation by diffusion for time-resolved macromolecular crystallography. *Adv Cond Matter Phys* 167276.

Schotte, F., Cho, H.S., Kaila, V.R., Kamikubo, H., Dashdorj, N., Henry, E.R., Graber, T.J., Henning, R., Wulff, M., Hummer, G., Kataoka, M., Anfinrud, P.A. (2012). Watching a signaling protein function in real time via 100-ps time-resolved Laue crystallography. *Proc Natl Acad Sci USA* **109**, 19256-19261.

Schotte, F., Lim, M., Jackson, T.A., Smirnov, A.V., Soman, J., Olson, J.S., Phillips, G.N. Jr,, Wulff, M., Anfinrud, P.A. (2003). Watching a protein as it functions with 150-ps time-resolved X-ray crystallography. *Science* **300**, 1944-1947.

Sierra, R.G., Laksmono, H., Kern, J., Tran, R., Hattne, J., Alonso-Mori, R., Lassalle-Kaiser, B., Glöckner, C., Hellmich, J., Schafer, D.W., Echols, N., Gildea, R.J., Grosse-Kunstleve, R.W., Sellberg, J., McQueen, TA., et al. (2012) Nanoflow electrospinning serial femtosecond crystallography. *Acta Crystallogr D Biol Crystallogr* **68**, 1584-1587.

Spence, J.C., Weierstall, U., and Chapman, H.N. (2012). X-ray lasers for structural and dynamic biology. *Rep Prog Phys 75*, 102601.

Spence, J.C. (2017). XFELs for structure and dynamics in biology. *IUCr J* **4**, 322–339.

Stagno, J.R., Liu, Y., Bhandari, Y.R., Conrad, C.E., Panja, S., Swain, M., Fan, L., Nelson, G., Li, C., Wendel, D.R., White, T.A., Coe, J.D., Wiedorn, M.O., Knoska, J., Oberthuer, D., et al. (2017). Structures of riboswitch RNA reaction states by mix-and-inject XFEL serial crystallography. *Nature* **541**, 242-246.

Suga, M., Akita, F., Sugahara, M., Kubo, M., Nakajima, Y., Nakane, T., Yamashita, K., Umena, Y., Nakabayashi, M., Yamane, T., Nakano, T.,

Suzuki, M., Masuda, T., Inoue, S., Kimura, T., et al. (2017). Light-induced structural changes and the site of O=O bond formation in PSII caught by XFEL. *Nature* **543**, 131-135.

Sugahara, M., Mizohata, E., Nango, E., Suzuki, M., Tanaka, T., Masuda, T., Tanaka, R., Shimamura, T., Tanaka, Y., Suno, C., Ihara, K., Pan, D., Kakinouchi, K., Sugiyama, S., Murata, M., et al. (2015). Grease matrix as a versatile carrier of proteins for serial crystallography. *Nat Methods* **12**, 61-63.

Sugahara, M., Nakane, T., Masuda, T., Suzuki, M., Inoue, S., Song, C., Tanaka, R., Nakatsu, T., Mizohata, E., Yumoto, F., Tono, K., Joti, Y., Kameshima, T., Hatsui, T., Yabashi, M., et al. (2017). Hydroxyethyl cellulose matrix applied to serial crystallography. *Sci Rep* **7**, 703.

Tenboer, J., Basu, S., Zatsepin, N., Pande, K., Milathianaki, D., Frank, M., Hunter, M., Boutet, S., Williams, G.J., Koglin, J.E., Oberthuer, D., Heymann, M., Kupitz, C., Conrad, C., Coe, J., et al. (2014). Time-resolved serial crystallography captures high-resolution intermediates of photoactive yellow protein. *Science* **346**, 1242-1246.

Tosha, T., Nomura, T., Nishida, T., Saeki, N., Okubayashi, K., Yamagiwa, R., Sugahara, M., Nakane, T., Yamashita, K., Hirata, K., Ueno, G., Kimura, T., Hisano, T., Muramoto, K., Sawai, H., et al. (2017). Capturing an initial intermediate during the P450nor enzymatic reaction using time-resolved XFEL crystallography and caged-substrate. *Nat Comms* **8**, 1585.

Tschentscher, T., Bressler, C., Grünert, J., Madsen, A., Mancuso, A., Meyer, M., Scherz, A., Sinn, H., Zastrau, U. et al. (2017). Photon Beam Transport and Scientific Instruments at the European XFEL. *Appl Sci* **7**, 592-535.

Vivien, Marx. (2017). Structural biology: doors open at the European XFEL. *Nat Methods* **14**, 843.

Wallace, E., Dranow, D., Laible, P.D., Christensen, J., and Nollert, P. (2011). Monoolein Lipid Phases as Incorporation and Enrichment Materials for Membrane Protein Crystallization. *PLoS ONE* **6**, e24488.

Wang, D., Weierstall, U., Pollack, L., and Spence, J. (2014). Double-focusing mixing jet for XFEL study of chemical kinetics. *J Synchroton Rad* **21**, 1364-1366.

Weierstall, U., James, D., Wang, C., White, T.A., Wang, D., Liu, W., Spence, J.C., Bruce Doak, R., Nelson, G., Fromme, P., Fromme, R., Grotjohann, I., Kupitz, C., Zatsepin, N.A., Liu, H., et al. (2014). Lipidic cubic phase injector facilitates membrane protein serial femtosecond crystallography. *Nat Commun* **5**, 3309.

Yabashi, M., Tanaka, H., Tono, K., and Ishikawa, T. (2017). Status of the SACLA Facility. *Appl Sci* **7**, 604-610.

Young, I.D., Ibrahim, M., Chatterjee, R., Gul, S., Fuller, F., Koroidov, S., Brewster, A.S., Tran, R., Alonso-Mori, R., Kroll, T., Michels-Clark, T., Laksmono, H., Sierra, R.G., Stan, C.A., Hussein, R., et al. (2016). Structure of photosystem II and substrate binding at room temperature. *Nature* **540**, 453-457.